Strathprints Institutional Repository

Machining Based Coverage Path Planning for Automated Structural Inspection

Charles Norman Macleod, Gordon Dobie, Stephen Gareth Pierce, Rahul Summan, Maxim Morozov

Abstract—The automation of robotically delivered Non Destructive Evaluation (NDE) inspection shares many aims with traditional manufacture machining. This paper presents a new hardware and software system for automated thickness mapping of large-scale areas, with multiple obstacles, by employing CAD/CAM inspired path planning to implement control of a novel mobile robotic thickness mapping inspection vehicle. A custom post-processor provides the necessary translation from CAM Numeric Code through to robotic kinematic control to combine and automate the overall process. The generalised steps to implement this approach for any mobile robotic platform are presented herein and applied, in this instance, to a novel thickness mapping crawler. The inspection capabilities of the system were evaluated on an indoor mock-inspection scenario, within a motion tracking cell, to provide quantitative performance figures for positional accuracy. Multiple thickness defects simulating corrosion features on a steel sample plate were combined with obstacles to be avoided during the inspection. A minimum thickness mapping error of 0.21 mm and mean path error of 4.41 mm were observed for a 2 m^2 carbon steel sample of 10 mm nominal thickness.

The potential of this automated approach has benefits in terms of repeatability of area coverage, obstacle avoidance and reduced path overlap, all of which directly lead to increased task efficiency and reduced inspection time of large structural assets.

Note to Practitioners— Current industrial robotic inspection approaches largely consist of manual control of robotic platform motion to desired points, with the aim of producing an number of straight scans for larger areas, often spaced meters apart. Structures featuring large surface area and multiple obstacles, are routinely inspected with such manual approaches, which are both labour intensive, error prone and do not guarantee acquisition of full area coverage.

The presented system addresses these limitations through a combined hardware and software approach. Core to the operation of the system is a fully wireless, differential drive crawler with integrated active ultrasonic wheel probe, to provide remote thickness mapping. Automation of path generation algorithms is produced using commercial CAD/CAM software algorithms, and this paper sets out an adaptable methodology for producing a custom post-processor to convert the exported G-Codes to suitable kinematic commands for mobile robotic platforms. The differential drive crawler is used in this paper to demonstrate the process. This approach has benefits in terms of improved industrial standardisation and operational repeatability.

The inspection capabilities of the system were documented on an indoor mock-inspection scenario, within a motion tracking cell to provide quantitative performance figures for the approach. Future work is required to integrate on-board positioning strategies, removing the dependency on global systems, for full automated deployment capability.

Index Terms— Automated Coverage Path Planning, Automated Robotic Inspection, Automated NDE, CAD/CAM Based Path Planning.

I. INTRODUCTION

With a concerted and growing emphasis on human safety [1] and the environment [2], greater information is required on the current state and condition of the world infrastructure. Higher operational demands such as greater working loads and longer working lifetimes [3], coupled to reduced capital investment in replacement designs, has exerted greater strain and stress on numerous components critically affecting their condition and safe working lifetime [4].

To ensure that infrastructure owners, operators and planners have sufficient information readily available to them regarding the state and condition of their asset, numerous advances and developments have been demonstrated in the field of Non Destructive Evaluation (NDE). The process of detailed imaging and examination of structures in a sensitive, safe and inherently non-intrusive manner has numerous advantages in operational, financial and safety terms. Quantitative information on the condition of parts and components, allow skilled personnel or emerging automated approaches to make decisions on remaining lifetime and required replacement, ensuring maximum asset value, usage and safety.

Numerous applications requiring inspection on large scale structures, such as those found in the energy sector, are often in areas difficult to access and hazardous to human beings [4]. This, along with the requirements for greater inspection accuracy and efficiency has underpinned a research and development drive to automate current NDE inspection techniques [4,5]. Only by delivering NDE inspection systems to all points of interest within a structure, can full-scale coverage of the assembly be undertaken. There exists a drive to ensure full coverage to ensure no defects are overlooked or neglected. Automation of such inspection procedures improves accuracy by reducing human error [6], which can

often be categorised as the weakest link in the NDE supply chain [7]. Task efficiency and completion times can potentially be further improved through employment of a swarm of autonomous intelligent systems. Furthermore automated processing of collected NDE sensor data can then be undertaken to aid defect detection and recognition, especially when dealing with large sensor datasets [8].

The requirement for autonomous NDE systems has driven research and development in robotic inspection platforms capable of accessing structures and undertaking NDE using specialised sensors [9]. Previous research within the Centre for Ultrasonic Engineering (CUE) (University of Strathclyde) has focussed on mobile crawlers [4,9], localisation strategies and approaches through novel visual [10] and Bayesian methods [11], along with multi sensor (Ultrasonic, Visual and Magnetic Flux Leakage (MFL)) payload delivery [12-14]. Similarly inspired research has been undertaken internationally focussing on areas such as robot design [15-16], path planning for crawlers [5,17-18] and component inspection [19-20]. All path-planning approaches described in [5,17-18] fundamentally design their method for optical or visual inspection deployment techniques, which coincidentally only perform surface inspection and do not perform internal imaging. Internal imaging of structures, such as thickness mapping, is commonly undertaken using ultrasonic techniques which require consistent control of sensor-to-surface normality and typically feature a very much reduced single-point measurement inspection volume when compared to visual sensors. The genetic algorithm [5], spanning-tree [17] and Voronoi [18] path planning algorithms presented do not therefore naturally directly translate to automated internal imaging and ultrasonic thickness mapping applications.

Current industrial state-of-the-art large-area asset remote thickness mapping inspection approaches largely consist of full manual remote control of a robotic delivery platform with an integrated ultrasonic sensor. The operator manually controls platform motion to desired points, with the aim of producing a number of straight scans for larger areas, often spaced meters apart. Structures such as oil storage tanks, featuring large surface areas and multiple access hatch obstacles, are routinely inspected with such approaches and can take up to a number of days to inspect in such a labour intensive manner, while still not acquiring full area scanning coverage [21-23].

This paper presents contributions to the field of automated inspection of large-scale assets, building on the current technology and the level presented above. Such contributions, most notably, relate to a new adaptation of an automated path planning strategy, platform design, robot control and data processing. Firstly, a core contribution presented herein is a software pipeline for performing coverage path planning, especially suited for internal imaging and thickness mapping inspections. Built upon traditional CAD/CAM operations and introduced for the first time for automated mobile robot inspection applications, this approach is applicable to many mobile robotic devices. A second core contribution is

introduced through a proof-of-concept demonstration of a simulated inspection scenario. This is undertaken using a custom novel robotic inspection platform which allows for the characterisation of complete system performance.

Section II details path planning concepts, with a focus on inspection related approaches, highlighting similarities between such NDE application areas and traditional machining operations. Section III introduces the hardware, firmware and software developed for this body of work. Section IV details the technical structure of the proof-of-concept demonstration, utilised to undertake a mock industrial inspection. The subsequent proof-of-concept demonstration characterisation results are introduced and analysed in Section V. Section VI concludes the paper and notes future areas of relevant work.

II. PATH PLANNING

For remote inspection procedures to achieve greater coverage and efficiency, fundamental changes in the approach of both current delivery platforms and their associated control and path planning systems are required. Automated path planning must be introduced to replace traditional inefficient manual approaches. Path generation algorithms produce the necessary waypoints and trajectories for automated travel of the platform and deployment of sensors to the points of interest. Path planning strategies must account for desired area and volume coverage while also ensuring obstacle avoidance. Additionally they must consider and ensure both safe access and exit of the complete system.

A. Coverage Path Planning

Coverage Path Planning (CPP) is the procedure of determining a path that passes over all points of an area or volume while avoiding obstacles [24]. Example robotic applications that fundamentally require such a planning strategy include vacuum cleaning robots, painting robots, underwater imaging systems, demining robots, lawn mowers, agricultural robots and window cleaners [25-28]. Cao et al [28] defined a set of criteria and requirements for robotic systems undertaking CPP operations in 2D environments.

1. The robot must move through all the points in the target area covering it completely.
2. The robot must inherently have the ability to fill the region without overlapping paths.
3. Continuous and sequential operation without any repetition of path is required
4. The robot must avoid all obstacles
5. Simple motion trajectories (e.g. straight lines or circles) should be used for simplicity and control.
6. An "optimal" path is desired under available conditions.

CPP algorithms can be classified as heuristic or complete depending on whether or not they provably guarantee complete coverage of the free space [24]. Additionally they can also be classified as either off or on-line. Off-line

programming requires *a priori* knowledge of the environment and it remaining static throughout the operation window [29], while on-line algorithms feature no *a priori* knowledge and utilise real-time sensor measurements to profile the environment and path plan based on the acquired information.

Automation of path planning can yield benefits in terms of production, efficiency, and safety. The industry application which has received considerable research and industrial focus in automated area CPP, is that of spray painting [30]. More recently CPP for industrial component inspection has undergone significant research in high value manufacturing applications, especially in aerospace, with a variety of NDE sensors being deployed [20,31-35]. Internal imaging applications in the manufacturing sector have utilised conventional robot arms to ensure sensor-to-surface normality and [20,35] present a CAD/CAM inspired path-planning toolbox for such robot deployment mechanisms.

CPP for crawler devices has also recently attracted research interest in areas such as material handling and logistics [36], vacuum cleaners, agriculture [37], demining [27] and inspection [5,17,18,33-34], Traditional path planning algorithms for such platforms has focussed on Configuration Space (C-Space) representations such as Voronoi diagram [38], regular & occupancy grids, generalised cones [39], quad-tree [40] and vertex graphs. Additionally CPP for Aerial platforms has received attention for opportunities in surveillance [41], agriculture [42] and disaster and emergency management.

B. Inspection path planning

Although sharing similarities to other industrial robotic application CPP strategies, automated inspection CPP is further challenging insofar that typical NDE applications require scanning of features that would normally be classed as obstacles in traditional robotics. This subtle distinction must be considered, as robotic positioning and path planning algorithms must not safely avoid such an object, by traditionally moving as far as possible away from the object, but carefully approach such objects to allow NDE sensors to be deployed with very precise sensor-surface stand-off distance control. Stand-off distance must be consistent, along or around such objects, while also being repeatable, to allow industry code compliant inspection strategies to be deployed at regular intervals. This latter point ensures operators are able to confidently monitor rate of change of inspected structures.

Automated identification and selection of such features requiring inspection, for enhanced throughput and automation is very much in its infancy [35] and is not considered in this body of work. Avoidance strategies must not only recognise obstacles, but also be intelligent in determining them as features requiring inspection, or in fact just obstacles requiring avoidance. Therefore a future requirement would be to group objects into those that require inspection and those requiring avoidance.

One critical exception to traditional object avoidance strategies and of significance to automated NDE systems is when deploying contact based traction platforms. Crawler platforms such as wheeled or gripper clamps, deploying traditional ferromagnetic/friction strategies or more advanced approaches such as vacuum devices [43], use surfaces for successful manoeuvring. Additionally such strategies must also consider the platform propulsion technique and its requirements when deciding courses of action.

It is therefore logical that all parts of an automated NDE system, except contact based inspection/localisation sensors and traction devices, should always avoid contact to nearby objects throughout the inspection process. This is highly applicable in deployment strategies of tight space or confined access, en-route to a desired inspection point.

C. Inspection Path Planning Parameters

Path or motion planning is a key component in the realisation of autonomous robotic systems [44]. From a robotic perspective, path planning is the method and approach to progress to a defined goal or location. Interlinked and conflicting parameters such as obstacle avoidance, velocity, completion time and robustness define the overall strategy and technique. These are discussed in greater detail below, highlighting the key parameters of inspection path planning:

1) Deployment Platform Design

The deployment platform dictates the optimum path planning strategy to be investigated. Full 6 D.O.F. platforms (aerial, conventional robot arms) can naturally manoeuvre to positions along paths that low D.O.F rail constrained scanners and surface traction platforms (crawlers) cannot achieve. This additional freedom allows greater flexibility dealing with challenging access constraints albeit at the expense of obstacle avoidance.

2) Area & geometry to be inspected & imaged

The area, point or object requiring inspection naturally dictates the path planning strategy. For example simple flat rectangular geometries would typically require traditional parallel raster scanning techniques, while spiral geometries would require circular loop paths. Complex shaped surfaces naturally require complex spline type paths.

3) Inspection Sensor

When considering path step-over, of critical importance is the sensor active aperture or sensor footprint. The sensor choice and area to be inspected are closely interlinked insofar that they directly dictate the number of imaging passes required to completely satisfy the coverage requirements. Sensor resolution is controlled by design fundamentals and relates to the window and sampling area of the sensor.

4) Inspection Path Pattern

The NDE path pattern is directly dictated by parameters such as inspection speed and desired resolution. Firstly, the sampling time of traditional NDE sensors defines the maximum motion velocity which directly limits the overall inspection time. Path resolution is dictated by the largest spacing increment between subsequent waypoints, while measurement resolution is fundamentally limited by the maximum sensor and path resolution. Additionally overall

inspection time is directly controlled by the motion velocity and measurement spacing along the desired path.

5) Platform & Sensor Positioning Strategies

The precision, accuracy and repeatability of the platform and sensor positioning system ultimately limit the maximum inspection coverage rate, as inaccuracies would yield greater required path overlap and multiple sweeps. Additionally the initial tolerance of any acquired surface/object metrology information can affect the coverage rate as multiple incremental sweeps may be required to image the feature.

6) Material & Surface Properties

The material under inspection can influence the path planning strategy in two distinct manners. Firstly, the delivery platform may use a particular method of traction (e.g. magnetic) and restrict its movement to surfaces that suit such constraints. Secondly, the material itself may dictate the pose of the NDE sensor to very specific values or ranges, depending on parameters such as surface roughness or local geometry.

D. Inspection & Machining Path Planning Parallels

The automation of traditional machining operations began with Numeric Control (NC) in 1952 [45]. NC offered control of mechanical actuators, through electronic commands. The advent of Computer Numeric Control (CNC) allowed more complex multi-axis machining tool paths to be generated efficiently and safely [46,47].

It is identified herein that both automated inspection and traditional machining path planning, share many common aims and goals. Firstly, they both desire to efficiently fully cover large areas of both planar and complex geometry while retaining sensor-to-surface normality of the tool/sensor. Additionally, both scenarios can feature boundaries and areas that are to be left untouched. Furthermore each application can require singular paths around distinct components of both simple and complex nature.

The individual concepts of manufacturing path planning, for milling operations, are considered below along with the corresponding parallels to NDE inspection concepts. Table 1 summarises the equivalent parameters.

1) Manufacturing Process Planning

This considers the overall process and flow of undertaking milling operations. Similarly, in automated inspection applications such planning is undertaken to maximise asset or component utilisation or value. Such an inspection example scenario would include that of a storage vessel inspection, which would likely require draining, prepared accordingly and then inspected, prior to painting and return to service.

2) Machine Tool and Controller Hardware Design Kinematics.

This considers the physical capabilities, in terms of speeds, acceleration and range of movements which can be achieved by the machine tool. In an automated NDE context this relates to the deployment platform design, its degrees of freedom, its controller and positioning feedback strategies

3) Cutting Parameter Estimates and Modelling

In traditional machining operations, parameters such as cutting force and travel velocities, are highly dependent on the material, cutting tool, desired throughput and machine rigidity. Optimisation allows operators to specify maximum safe permissible cutting parameters for maximum throughput feed rates. Similarly in an inspection context, the sensor defines parameters such as contact pressure, maximum travel velocity and sampling window. Additionally, the surface and geometry to be inspected, along with the platform design and control strategies, define travel velocities and accelerations, especially with surface contact traction devices.

4) Path Generation

Manufacturing operations require the efficient movement of the cutter across the areas and features requiring machining. Similarly NDE sensors require to be scanned in a repeatable and precise fashion across areas requiring inspection.

5) Machining Simulation and Verification

To allow operators to visualise and proceed with machining operations, simulation of the tool cutter with respect to the machined part is typically performed. This ensures the final part is as manufactured with no errors, produced by stray cutting operations, while also allowing the operator to plan the physical process around items such as fixturing and cycle time. In automated NDE applications, such simulations offer the operator the opportunity to ensure compliance with the required feature coverage while also ensuring no collisions with the sample or surroundings.

Path Planning Equivalent Parameters					
Machining	Manufacturing Process Planning	Machine tool and Controller Hardware Design Kinematics.	Cutting Parameter Estimates and Modelling	Path Generation	Machining Simulation and Verification
Equivalent Parameter	↕	↕	↕	↕	↕
Automated Inspection	Inspection Process Planning	Deployment Platform Design / Platform & Sensor Positioning Strategies	Inspection Sensor / Material & Surface Properties / Deployment Platform Design	Inspection Path Pattern	Inspection Simulation and Verification

Table 1. Illustrated are the equivalent and comparable parameters of Machining and Automated Inspection path planning.

E. Traditional Machining: Pocket milling

In typical negative machining operations a pocket is defined as an area with defined borders in which material should be removed. It must be noted that the borders can be defined inside or outside the part denoting a closed or open pocket respectively [42]. Additionally, island units are defined as areas that are to be left un-machined and avoided (Fig. 1). Such path operations are generated using the Configuration Space methods descibed in [49,50]. Such operations share strong similarities to many common NDE inspection scanning scenarios, where areas are desired to be scanned with raster scan paths while avoiding obstacles.
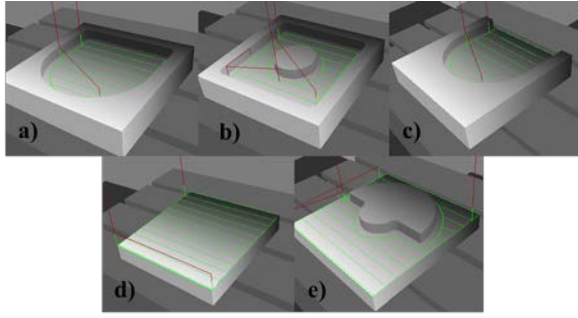
Fig. 1. a) Closed Pockets, b) Closed Pockets with Island, c) d) Open Pocket with Bounds, e) Completely open pocket, f) Open pocket with Island [48]. Illustrated is the varying pocket milling machining operation for each case.

F. Machine Control and Implementation

The industrial standard for machine tool operation through Computer Aided Manufacturing (CAM) techniques is that of G-Code [51]. G-Code is a standardised high level NC language that is accepted by all standard CNC machine tools. Movements such as straight line (G01) and arc interpolations (G02,G03) are standard operations along with control of plunge-rate, feed-rate and spindle speed. These basic functions allow a variety of operations to be undertaken and machining functions to be then performed. Additional G-Code functions have been added to the standard protocol which allow more complex operations to be performed.

1) Post-Processors

A post-processor is a tool that translates output statements from a robot simulator to a target robot language (G-Code), for deployment of off-line path planning programming algorithms [52,53]. Post processors can be categorised as system-dependent, application dependent or generic [53]. System dependant post-processors translate robot simulation commands into a specific robot language, traditionally applicable to a certain manufacturer or system protocol [54]. Application dependant post-processors are made for a specific application with custom sequences. Generic post-processors are theoretically capable of translating multiple simulator commands into languages for multiple robot controllers [53].

III. OVERALL SYSTEM DESIGN

To evaluate and highlight the scalable benefits of machining based path planning for automated structural inspection a comprehensive suite of hardware and software was developed.

Firstly, a novel ultrasonic sensing inspection platform the Automated Ultrasonic Thickness (AUT) Remote Sensing Agent (RSA) was adapted and optimised, building on previous work [55], to investigate the feasibility of multiple obstacle automated inspection.

Secondly, a software pipeline was developed, utilising both commercial and custom developed packages to undertake and highlight coverage path planning for automated inspection applications. The overall system structure and flow is shown below in Figure 2.

Commercial CAD/CAM software was used to generate machining path trajectories, while a custom post-processor

and control and processing packages were developed specifically for this body of work and the AUT RSA, in an established custom software package (RSA GUI) [4]
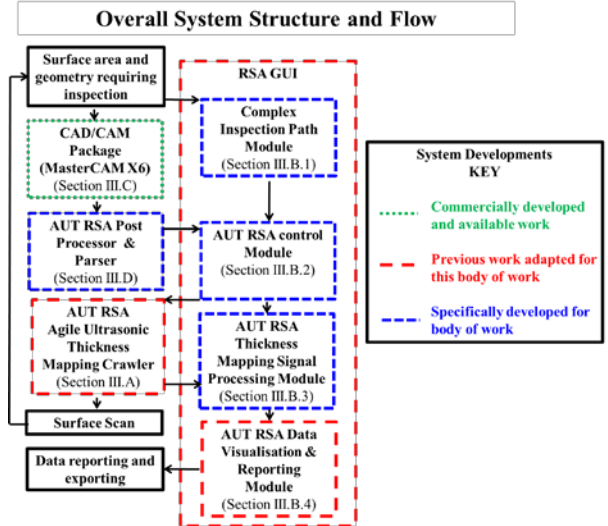

Fig. 2. Overall System Structure and Flow. Highlighted is the detailed breakdown of commercially developed, previously developed and newly developed work, with direct reference to their corresponding relevant section in the manuscript.

A. AUT RSA Hardware

The AUT RSA is a recently developed three wheel robotic crawler featuring the novel step of a single element ultrasonic wheel probe fitted as an active rear wheel (Fig. 3a). Introduced in [55] and revised, for this body of work, the crawler design allowed for versatile steering and accurate dead reckoning of the platform, which is not feasible with industrial four wheeled designs due to their requirement of slippage when turning. These unique characteristics allow the platform an unrivalled degree of mobility when compared to traditional NDE crawler inspection platforms. The fully wireless nature of the platform offers advantages when compared to current wired based systems, which are limited in their overall reach and deployment suitability when considering umbilical dynamics, mass and tangle free operation. The AUT RSA platform featuring magnetic traction therefore significantly widens the scope and potential of automated full area coverage thickness mapping.

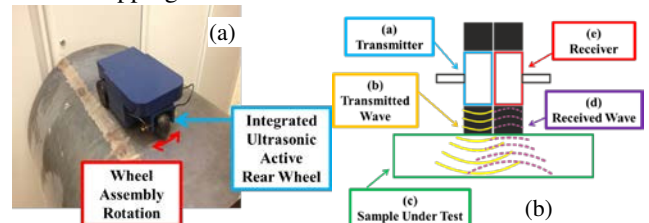**Fig. 3. AUT RSA (a) and wheel probe illustration (b). Figure 3b highlights the sound wave propagation from transmitter, through the tyre to sample and back to receiver.**

The wheel probe was a Silverwing NDT 5 MHz split crystal dry coupled sensor. Featuring no liquid filled region it consists of two solid acoustically matched rubber tyres rotating around a transducer housing to allow propagation of the transmitted

compressional wave and receive signals respectively (Fig. 3b). The wheel probe has an approximate horizontal minimum spatial resolution of 24 mm.

The integrated drive electronics consisted of a custom single channel high voltage square wave pulser. A boost DC-DC convertor provided a 110V drive excitation voltage. Newly developed acquisition electronics, for enhanced signal recovery, consisted of a custom implemented single channel low-noise pre amplifier (AD8015 & AD8370 [56]) coupled to a high speed Field Programmable Gate Array (FPGA) Analogue to Digital Convertor (ADC) [57]. A USB connection established with the on-board General Purpose Processor (GPP), allowed buffering and transferring of raw data to the host computer (Fig. 4.)

Fig. 4. Newly Developed Ultrasonic Acquisition Structure. All ultrasonic data, and co-incidentally all robot variables, are transferred wirelessly back to a computer base station GUI.

Positional tracking and feedback control of the AUT RSA within the laboratory volume was achieved using a VICON Six Degree of Freedom (D.O.F.) Motion Capture System (VMCS) [58]. This photogrammetry system utilises multiple optical cameras to track the pose of a unique arrangement of retro-reflective markers attached to the platform.

1) AUT RSA Firmware

New low-level firmware, stored on an embedded microcontroller, was specifically developed for control of the active rear wheel. A Proportional Derivative (PD) controller was implemented to ensure the rotation angle of the rear wheel matched the desired angle and that of the result of the two front wheels differential. The controller was manually tuned to ensure a suitable response profile and minimum overshoot.

B. RSA GUI

Additional software packages were developed and current packages modified within an established custom C++ Personal Computer (PC) RSA Graphical User Interface (GUI) for full control of the AUT RSA.

The GUI features a 3D visual world representation, where structural asset Computer Aided Drawing (CAD) models can be imported, displayed and the position of the robot relative to the sample visualised. Path trajectories can be manually selected across the sample and subsequent NDE results can be displayed and visualised relative to the sample. All RSA parameters including raw NDE results are logged and can be visualised live if desired.

1) Complex Inspection Path Module

This package allowed complex shaped surfaces and geometries to be imported into the 3D visual world. This feature allowed subsequent desired path planning algorithms and results to be overlaid and displayed on the inspection geometry.

2) AUT RSA Control Module

This module featured the necessary functions and parameter settings, such as wheel velocity and pose, to allow control and optimisation of the additional D.O.F found on the AUT RSA with its active rear wheel. This module also included a manually tuned PID heading controller, with positional information measured by the VMCS, to maintain path following and attain desired waypoints.

3) AUT RSA Thickness Mapping Signal Processing Module

All captured raw ultrasonic signals were wirelessly transferred to the remote RSA GUI. Due to the compressive nature of the wheel probe tyre and the variation in sound propagation through the tyre and sample, accurate calculation of the thickness of the sample based on conventional time of flight information between the transmitted pulse and the first back-wall echo return was deemed unsuitable. Therefore the corresponding thickness of the material was calculated using successive back-wall echos, with three successive echos utilised for averaging purposes. Additionally small local variations in coupling between tyre and surface yield corresponding change in back wall echo amplitude, with poorly coupled instances yielding reduced amplitudes. The minimum peak detection amplitude of each back wall echo must therefore take into consideration the coupling environment. As the receive acquisition process begins shortly after the firing pulse, the largest peak in the acquired captured data logically corresponds to the first back wall echo. Due to the attenuative nature of traditional materials successive back wall echoes have correspondingly reduced amplitudes. The peak detection algorithm (1) therefore accounted for variation in the amplitude of the first echo and detection of both the second and third maxima based on the former (Fig. 5).
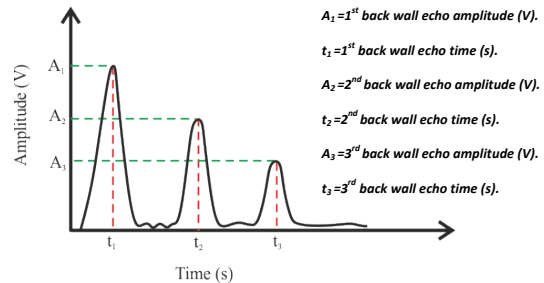
Fig. 5. Back Wall Echo Thickness Measurement. Successive wall reflections are utilised for averaging purposes to determine sample material thickness

$$m_t = \left(\frac{v_c \times (t_3 - t_1)}{4} \right) \qquad (1)$$

Where m_t =Material thickness (mm) and v_c =Speed of sound in material (mm/s). Each ultrasonic acquisition was both time and position-stamped. The position of the AUT RSA as measured by the VMCS, was that of the centre of turning rotation, namely the central point of the front two drive wheels. As the wheel probe was located at the rear of the platform, displaced in one axis along the length of the robot,

the position of the actual ultrasonic measurement followed an arc movement centred on the RSA centre of rotation. A 2D coordinate transform was utilised to calculate the point of ultrasonic measurement as shown in (2,3) where Ψ_{RSA} equals the yaw angle (°) of the AUT RSA as measured by the VMCS, D_{TTC} the distance (mm) from the transducer to AUT RSA turning centre and RSA_{TCx}, RSA_{TCy} represent the VMCS measured turning centre positions.

$$UT\_Meas\_Pos_x = (D_{TTC} \times \cos\Psi_{RSA}) + RSA_{TCx} \quad (2)$$
$$UT\_Meas\_Pos_y = (D_{TTC} \times \sin\Psi_{RSA}) + RSA_{TCy} \quad (3)$$

Therefore all ultrasonic measurements were recorded at their correct position of capture.

4) AUT RSA Data Visualisation & Reporting Module
A new module for results visualisation and processing was implemented within MATLAB, but able to be called from the RSA GUI. This package allowed the previous inspection geometry to be exported and all scan data, including thickness data and sensor scan paths to be overlaid on the geometry. Additionally this module allows quantifiable results to be obtained on parameters such as thickness deviation to original and sensor path error.

C. CAD/CAM Package

The Mastercam X6 package was utilised for CAM operations and subsequent machining inspired path trajectories.

1) Custom AUT RSA Machine Tool
A custom machine tool was designed within Mastercam to simulate the AUT RSA when undertaking an inspection operation (Table 2). The working envelope of the AUT RSA was represented as a cylinder of diameter 460 mm. This was calculated from the turning centre origin between the drive wheels to the safe outer maximum limit of extension of any part of the platform. This included the whole case, the active back wheel in all orientations and all associated connectors. Additional parameters were specified in relation to deployment velocities based on traditional speed and rate variables (Table 3).

Index	AUT RSA Parameter	Machine Tool Parameter (mm)
1	UT Wheel Probe Nominal Contact Area Diameter (20 mm)	Cutter Diameter
2	UT Wheel Probe Diameter (65 mm)	Flute Size
3	Wheel Probe Wheel Arch Nominal Height to Ground (73 mm)	Shoulder Size
4	AUT RSA Height (105 mm)	Overall Height
5	AUT RSA Working Envelope Diameter (460 mm)	Shank Diameter
6	AUT RSA Working Envelope Diameter (460 mm)	Holder Diameter
7	Holder Not Utilised - Nominal (1 mm)	Holder Height

Table 2. Highlighted are AUT RSA tool parameters and their equivalent machine tool parameter in the CAD/CAM environment.

AUT RSA Parameter	Machine Tool Parameter
RSA scanning speed (25 mm/s)	Feed Rate (mm per minute)
RSA travelling speed (50 mm/s)	Retract Rate (mm per minute)
RSA UT acquisition frequency (10 Hz)	Spindle Speed (revolutions per minute)

Table 3. Documented is the AUT RSA Auxiliary tool parameters and their corresponding equivalent machine tool parameter.

In 2D milling commands Mastercam features no intelligent tool collision protection by adaption of the path trajectory. It is a requirement of the operator to ensure no collisions occur by reviewing the generated path motion simulation. Due to the rear swing nature of the active back wheel of the AUT RSA, the full working envelope of the AUT RSA can, as discussed above, be defined with a radius of 230mm from the turning centre of the AUT RSA. The actual working envelope at any particular instance of time will consist of a partial section of the full envelope defined by the current pose of the platform. Therefore 230 mm of clearance around the contours of each island was specified to ensure no collisons.

D. AUT RSA Post-Processor

A custom system-dependent post processor and parser was developed for the AUT RSA to allow path trajectory algorithms to be simulated and deployed in inspection scenarios. The post processor was created to export only a limited number of basic function G-Codes (G01,G02,G03) and subsequently allow straight line and arc functions in a proof-of-concept demonstrator.

A parser was implemented within MATLAB to accept the post-processed numeric control (NC) output and convert this into suitable XML structured commands, as utilised for all desired paths and coordinates in the established RSA GUI. As all arcs are fundamentally represented by a finite number of straight-line sections, the parser first required the operator to specify the maximum length of any arc divided straight line sections. Each arc is was then divided into the corresponding number of straight-line interpolations from the start to the end of the arc.

E. AUT RSA Ultrasonic Calibration

The thickness mapping ability of the AUT RSA system was evaluated on a single straight-line path on a 10mm thick calibration sample plate (Carbon Steel S275 plate), 2000 mm long and 300 mm wide. A reference thickness measurement was taken ten times along the same path using a calibrated micrometer calliper. The result of this scan, with speed of sound set as 5920m/s, is shown in Table 4. To note is the small but consistent underestimate of sample thickness.

Parameter	Micrometer Value	AUT RSA Value	Error
Mean Thickness	9.98 mm	9.61 mm	-0.37 mm
Minimum Thickness	9.73 mm	8.86 mm	-0.87 mm
Maximum Thickness	10.21 mm	10.12 mm	-0.09 mm
Thickness Standard Deviation	0.15 mm	0.35 mm	0.2 mm

Table 4. AUT RSA ultrasonic thickness reference scan results with corresponding error characterisation against reference micrometer readings.

IV. PROOF-OF-CONCEPT DEMONSTRATION

Large steel plate structures are utilised in many industrial structures not limited to oil and gas storage tanks, ship hulls and wind turbine towers. Due to environment and local conditions these plates are often subject to corrosion and as

such gradually face loss of thickness. To confirm with appropriate legislation and ensure integrity, thickness mapping is periodically undertaken across the plated structure. Automated thickness mapping is a challenging inspection, when considering full area coverage, due to logistics such as structure features/obstructions, robotic logistics and environmental conditions.

The combination of the AUT RSA and machining based path planning approach yield themselves directly to the challenge of automated full area coverage inspection scanning. A sample, with typical obstacles and simulated defects was produced, to undertake a mock inspection scan and highlight proof-of-concept.

A. Industrial Sample

A sub-scale sample (2000 x 1000 x 10 mm Carbon Steel (S275) plate), including obstructions and simulated defects, was fabricated to mimic a traditional plated floor. Two obstructions were affixed to the plate to mimic typical industrial obstacles protruding through the floor (Table 5). Additionally seven flat bottom holes of 25 mm, all of varying depths, were machined into the underside of the plate at various locations to simulate localised loss of thickness (Fig. 6). The locations of these defects and their micrometer-measured depth are described in Table 6.

(a)

(b)
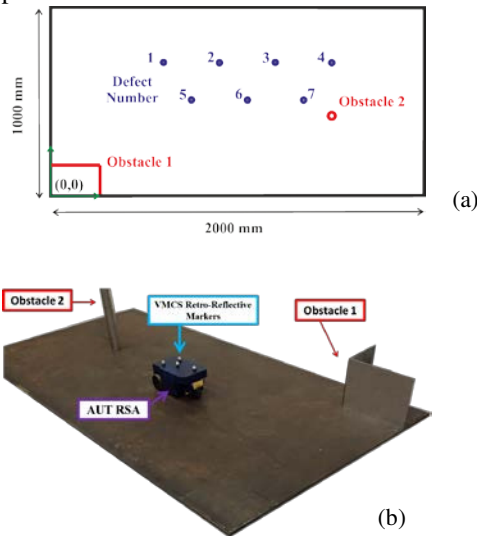
Fig. 6. Industrial Sample Diagram (a). Highlighted is the two top surface obstacles and seven bottom surface artificial defects. Photo of complete set-up and AUT RSA highlighted in (b)

| Obstacle Number	Description	Industrial Representation
1	Rectangular box of width 270 mm and breadth 170 mm, centred at (135, 85)	Pipe Duct
2	40mm Diameter Cylinder centred at (1500, 425)	Pipe Riser

Table 5. Industrial sample obstacle information with corresponding industrial component equivalent representation

Defect Number	Diameter (mm)	Location(x,y) (mm)	Micrometer Measured Plate Thickness (mm)
1	25	600,710	8.25
2	25	900,710	6.08
3	25	1200,710	3.85
4	25	1500,710	1.66
5	25	750,510	6.20
6	25	1050,510	3.74
7	25	1350,510	0.80

Table 6. Industrial sample artificial defect location information with corresponding reference micrometer thickness reading.

A manual ultrasonic thickness benchmark was conducted, prior to obstacle fitment, using standard equipment (5 MHz GE Roto-Array and Olympus Omniscan MX2). The reference thickness map is shown in Figure 7 highlighting the nominal 10 mm thickness and varying depth defects.
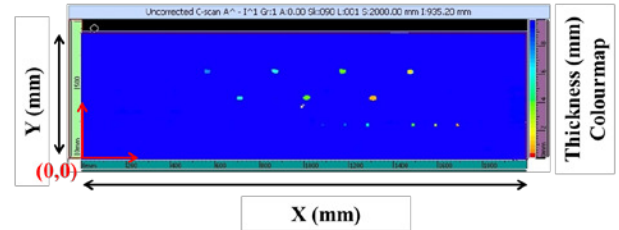

Fig. 7. Reference Industrial Thickness Map. Shown is the thickness change detected across all seven (25 mm diameter) defects, six (10mm diameter defects) and one non-artificial defect close to the plate centre.

All seven 25 mm diameter artificial defect flat-bottomed holes were located. Additionally a further defect was located nearby to defect 6, where on investigation of the surface area an adhesive film was found present which did not permit the ultrasonic wave to propagate through to the sample. An additional six 10 mm diameter holes present within the sample, near bottom centre right, but not related to this body of work, were also detected.

B. Automated Inspection Path Planning Strategy

To highlight proof-of-concept, a suitable measurement scanning strategy was developed. A raster scan with consistent spacing, across the sample, while avoiding the obstacles was deemed to highlight the benefits of this novel approach, especially when considering large-scale structures.

The CAD model of the industrial sample was produced in Mastercam to generate the appropriate numeric control output based on standard milling operations. The sample area was reduced to 1800 x 800 mm to allow safety margins for the robot. An open pocket with multiple island operations was selected with each island representing an obstacle. The desired stepover between paths was set to 50 mm, rather than the 10 mm minimum to ensure complete full area thickness mapping based on the transducer aperture area. This compromise was deemed justifiable and suitable in terms of coverage and task completion time, whilst still allowing scalability to the full value. The generated path, shown in Mastercam, is detailed below in Figure 8.
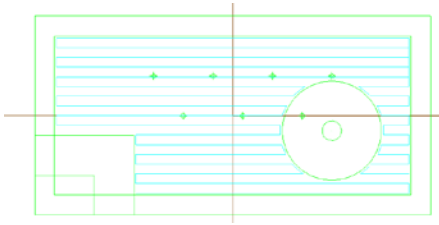
Fig. 8 Industrial Sample Scan Generated Path in Mastercam. Highlighted is the raster scan with 50 mm step-over and obstacle avoidance working envelope boundaries required to ensure no collisions when the AUT RSA is scanning.

The operation was then simulated to ensure no collisions and then exported through the CUE RSA post-processor and parser with a minimum arc interpolation distance of 10 mm selected. This was based on knowledge of the obstacle curvatures and the experience of the RSA drivetrain not being accurate on small distance motions due to the ramp-up phase of the motors [59].

The desired waypoints were then computed, exported into the RSA GUI and visually displayed for the operator, while offering the capacity to simulate the robot undertaking the scan path.

V. RESULTS AND DISCUSSION

1) NDE Results

The ultrasonic thickness map with superimposed defect outlines highlighting their location and size is shown in Figure 9. The result highlights the successful nature of the generated paths in avoiding both obstacles and simultaneously thickness mapping the sample. Run out areas from the steel sample perimeter, shown by the outer red lines at 2000 x 1000 mm, were manufactured from Medium Density Fibreboard at a similar height of 10 mm. The scan was undertaken in timeframe of 15 minutes.

Defect 1 was not fully detected as both path trajectories failed to intersect with the defect centreline. This underlined the importance of correctly defining both path scanning resolution, and minimum defect detection size to avoid loss of coverage events.
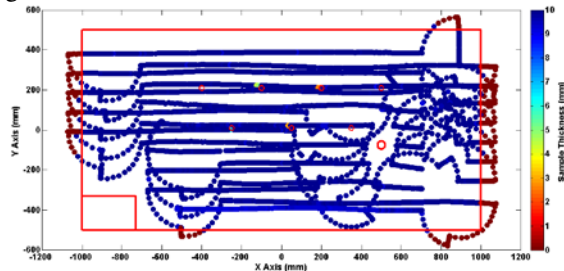
Fig. 9 AUT RSA Thickness Map with Overlaid Defects. Shown is the inbuilt obstacle avoidance ability of the strategy and the sample thickness measured at all scanned points and thickness changes detected near defects.

To visually identify potential defects all measurements with a recorded plate thickness lower than the minimum value obtained on the nominally similar calibration plate (8.86 mm),

were flagged and recorded as locations of potential loss of material. The result of this thresholding is shown below in Figure 10, again overlaid with superimposed defect outlines highlighting their location and size.
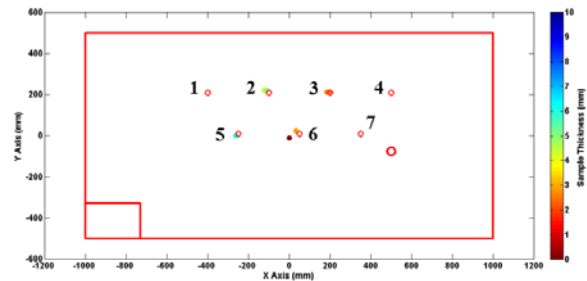
Fig. 10 AUT RSA Located Defects. Of particular note is the loss of thickness measured near artificial defects, 2,3,5 and 6.

Defects 4 and 7 were Not Detected (ND) due to the low nominal remaining plate thickness and the lightly damped characteristics of the transducer (Note, this was a limitation of the specific ultrasonic waveform characteristics employed rather than a fundamental limitation of the scanning technique). Defects 2, and 3 were all detected twice at neighbouring sample locations indicating that the AUT RSA transducer trajectory passed through the defect for more than one sample interval. Additionally one non-artificial defect was also located close to the plate origin, as previously highlighted by the reference ultrasonic thickness scan. The AUT RSA defect results are recorded in Table 7. The location of a measured defect was defined as the centre point of the transducer as calculated from platform turning centre position as measured by VMCS. The X and Y error was calculated from the difference between the actual position and the mean X and Y measured location when a defect was located by multiple measurements. When considering measured plate thickness the mean value was taken in instances of multiple successive measured plate thickness measurements.

Defect Number	Diameter (mm)	Actual Location (x,y) (mm)	Measured Location (x,y) (mm)	Error (x,y) (mm)	Actual Plate Thickness (mm)	Measured Plate Thickness (mm)	Plate Thickness Error (mm)
1	25	-400, 210	ND	N/A	8.25	ND	N/A
2	25	-100, 210	-124.4, 223.2 -112.3, 222.7	-18.35, 13.0	6.08	4.64	-1.44
3	25	200, 210	182.7, 213.2 194.8, 213.3	11.25, 3.3	3.85	2.57	-1.28
4	25	500, 210	ND	N/A	1.66	ND	N/A
5	25	-250, 10	-262.4, 1.2	-12.4, -8.8	6.20	5.99	-0.21
6	25	50, 10	32.2, 23.5	17.8, 13.5	3.74	2.82	-0.92
7	25	350, 10	ND	N/A	0.80	ND	N/A

Table 7 AUT RSA Scan Defect Information. Of particular note are columns, five and eight which indicate defect location error and subsequent plate thickness error respectively

The plate thickness error values noted above are clearly far away from the currently accepted convention of approximate accuracy limits (±0.002mm) when using modern equipment, manually scanned and calibrated for parameters such as cable lengths, temperature and surface properties [60]. However the values, shown in Table 7 are broadly aligned with the practical accuracy values of ±0.5mm, found in typical similar scenario manual inspections [61-63]. This is encouraging considering the automated aspect of the measurement and its relative

infancy.

Clearly as remaining plate thickness is obtained through time of flight measurement, a further calibration of plate velocity could be undertaken on the actual sample to better align the actual and measured results. As precision ultrasonic measurement was not the core focus of this body of work and the sensor platform was calibrated on a reference sample prior to deployment it was felt that this was unnecessary.

Fundamentally the ultrasonic thickness accuracy is a result of many parameters, such as the characteristics of the transducer receiver, instrument calibration, uniformity of material sound velocity and the performance of the automated thickness extraction algorithms.

The positional x,y error of each defect relies firstly on the pitch of the ultrasonic transducer, whereupon a smaller pitch will give a much reduced measurement aperture centred at a common point. Secondly, the error is dependent on the positional accuracy of the centre of the active back wheel mechanism, which itself is fundamentally dependant on the overall system path accuracy. This appreciation is critical to understanding the importance of overall platform and system path and position accuracy, which is detailed in the following section.

The current convention for desired probe position measurement accuracy, and in turn defect location position accuracy, is typically dependant on the application and techniques being deployed. In typical manual inspection applications < 1mm is desired, with some constrained geometry automated applications, typically using optimised low D.O.F Cartesian scanning rigs being far lower than this (±0.1mm) [64]. It must be noted the results from this novel implementation are further away from its manual counterpart than desired, but as stated are highly related to the platform path and pose accuracy which is now considered.

2) System Path Accuracy

To characterise the performance of the AUT RSA and quantify the path error for the scan, the desired and actual paths were compared. The 6 D.O.F. pose estimate, as measured by the VMCS, of the AUT RSA was sampled at a frequency of 50Hz. The path error at any individual VMCS measured point was defined as the perpendicular distance from the desired straight-line path to the VMCS measured point. The path accuracy statistical information is shown in Table 8. It is worth noting that both the large positive and negative path errors were encountered at corners or turning locations, while the lower mean and Root Mean Square (RMS) errors highlight the overall system performance, when considering the dominant straight-line path sections.

Parameter	Value
Max Path Error (Positive)	+13.48 mm
Max Path Error (Negative)	-19.38 mm
Mean Path Error (Absolute)	4.41 mm
RMS Error	6.14 mm
Path Error Standard Deviation	6.10 mm

Table 8 AUT RSA Path Accuracy.

The system path accuracy was dependent on many factors.

Firstly, the rigidity of the platform and the accuracy to which the zero degree angle of the active back wheel mechanism was first set and maintained. Secondly, the operation and performance of the AUT RSA pose heading controllers in controlling the platform pose along desired paths. Thirdly, the accuracy and resolution of the VMCS motion tracking system and the accuracy to which the VMCS object was defined initially with respect to the turning centre of the platform. It is the authors opinion that these were done to a sufficient standard to highlight the current state-of-the-art.

Previous studies of the XY mean squared path error encountered on a similar kinematic platform for NDE were found to be 7.10 mm at best, utilising an Extended Kalman Filter (EKF) and ultrasonic based tracking system, and 45.5 mm at worst using pure odometry from wheel encoders [11]. Such large error values were also observed in a motorised pipeline inspection robot utilising pure odometry [65], where the authors provided raw estimates of robot pose and hence defect location within an error range of 300 to 900 mm. Of particular note in [11] was that the path error was directly proportional to path length, and as found also in this body of work, the largest error deviations were located at turning points or corners.

To compensate for such errors, White et al. [66] highlighted that with the introduction of a manufacturing inspired interferometry based laser tracker (Leica LTD-800) positional accuracies as high as ±0.1mm can be obtained and as expected the accuracy of the crawler was highly dependent on the core accuracy of its pose measurement system. Work undertaken on characterising the accuracy of the VMCS was undertaken in [67] and highlighted it to be nominally > 1 mm, further highlighting the core accuracy limits achievable from the presented system and scan.

In [66] the laser tracker provided positional information, of a pan-tilt controlled retro-reflector, attached to an inspection crawler, into an EKF position and control strategy. It is worth noting that no detailed orientation accuracy was measured and that such equipment, while being of very high monetary value also requires full line of sight with the tracker base station at all times (often not a practically attainable constraint). With regards to the current body of work the authors believe that due to that due to afore-mentioned nature of obstacles in the inspection environment and the inherit ability to avoid these with the presented path planning strategy, it would be very challenging to ensure continuous line of sight during an inspection scan employing solely laser tracker based approaches. Future practical inspection systems will likely use tracking systems commensurate with the required application accuracy and suitability.

VI. CONCLUSION AND FUTURE WORK

The authors have presented a new comprehensive hardware and software solution for automated robotic NDE inspection scenarios. The new approach was demonstrated on a novel thickness mapping robot used to measure simulated corrosion wall thickness loss, in a steel sample plate representative of

many real inspection geometries.

The core hardware, critical to the realisation of the complete strategy, related to the development of the novel AUT RSA, a differential driven robot platform incorporating an actively driven rear ultrasonic wheel probe. The design allowed for versatile steering and accurate dead reckoning of the platform, while undertaking thickness mapping measurements, which is currently not feasible with industrial inspection platforms.

The similarities between traditional machining operations and NDE inspection path planning requirements were highlighted to be in areas including coverage efficiency, simulation and obstacle avoidance, while also in less-apparent areas such as path step-over and continuous sensor-to-surface normality requirements. A toolchain strategy was presented that allowed standard G-Code to be translated into the kinematic drive parameters for the mobile robotic inspection vehicle. The approach presented is quite general, relying on definition of robot platform specific kinematic parameters to achieve the correct G-Code post processing.

Utilisation of commercial machining path generation algorithms (in this example Mastercam) allowed the software system to be developed swiftly using an industry standard common language and methodology. This has commercial and operational benefits in providing a consistent and repeatable approach to path coverage, independent of individual NDE inspectors. Additional software was developed to acquire and process the raw ultrasonic measurement data to automatically produce a resultant thickness map.

The complete system was deployed on a mock industrial thickness mapping inspection scenario to highlight proof of principle and performance, with the results of this in terms of obstacle avoidance, ultrasonic thickness mapping and path accuracy presented and discussed. A minimum thickness mapping error of 0.21 mm and mean path error of 4.41 mm were observed for a 2 m^2 carbon steel sample of 10 mm nominal thickness. These results compare favourably with typical values obtained in related manual and robotic inspection scenarios.

In summary, such a demonstration and contributions improve and build-on the current state-of-the-art in large-scale-asset remote inspection and allow the potential for increased automation of the task with technical, commercial and safety benefits as described above.

Future work would investigate the addition and integration of on-board location sensor systems, while assessing their performance on parameters such as path accuracy, in an effort to remove global systems such as the VMCS for full remote automated inspection.

Furthermore, this new approach is not fundamentally limited to crawler platforms and could be scaled up to other platforms, such as aerial, by including the Z-Axis components of the CAM generated numeric code and combining with suitable kinematic model of the robotic platform in the post-processor. Therefore it can be conceived that the foundations to a scalable and flexible obstacle avoiding path planning strategy for robotic inspection applications have been presented.

REFERENCES

[1] HSE 'The Health and Safety of Great Britain' Health and Safety Executive 2009, http://www.hse.gov.uk/, Accessed Apr. 2014.

[2] SEPA 'Protecting Scotland's Environment – A 10 Year Perspective' Scottish Environmental Protection Agency, 2011.

[3] Ramírez, P. A. P. and Utne, I. B. 'Challenges due to aging plants', Process Safety Progress, vol. 30, issue 2, pp. 196–199, 2011.

[4] Dobie, G., Summan, R., Pierce, S. G., Galbraith, W. and Hayward, G., 'A noncontact ultrasonic platform for structural inspection' Sensors Journal, IEEE , vol.11, no.10, pp. 2458-2468, Oct. 2011.

[5] Lim, R.S.; Hung Manh La; Weihua Sheng, "A Robotic Crack Inspection and Mapping System for Bridge Deck Maintenance," Automation Science and Engineering, IEEE Transactions on , vol.11, no.2, pp.367,378, April 2014

[6] Hancock, P.A. and Chignell, M.H., , 'Mental workload dynamics in adaptive interface design', Systems, Man and Cybernetics, IEEE Transactions on , vol.18, no.4, pp.647-658, Jul. /Aug. 1988.

[7] Farley, J.M. and Babcock, M., 'Best Practice in the Application of NDT – An Update' In World Conference on NDT, 2004.

[8] Aldrin, J. C, Coughlin, C. R., Forsyth, D. S. and Welter, J. T., 'Progress on the Development of Automated Data Analysis Algorithms and Software for Ultrasonic Inspection of Composites' Review of Progress in Quantitative Nondestructive Evaluation (QNDE). Baltimore, Maryland, 2013.

[9] Friedrich, M., Dobie, G., Chan, C.C., Pierce, S.G., Galbraith, Marshall, W. S., and Hayward, G., 'Miniature Mobile Sensor Platforms for Condition Monitoring of Structures'. Sensors Journal, IEEE , vol.9, no.11, pp.1439-1448, Nov. 2009.

[10] Dobie, G., Summan, R., MacLeod, C.N. and Pierce, S.G., 'Visual odometry and image mosaicing for NDE'. NDT and E International, vol. 57, pp. 17-25, 2013

[11] Summan, R., Pierce, S.G., Dobie, G., Hensman, J. and MacLeod, C.N., 'Practical constraints on real time Bayesian filtering for NDE applications', Mechanical Systems and Signal Processing, vol. 42, issue 1-2, pp. 181-193. 2014.

[12] Dobie, G., Pierce, S. G. and Hayward, G., 'The feasibility of synthetic aperture guided wave imaging to a mobile sensor platform', NDT and E International, vol. 58. pp. 10-17, 2013.

[13] Dobie, G., Spencer, A., Burnham, K., Pierce, S. G., Worden, K., Galbraith, W. and Hayward, G. 'Simulation of ultrasonic lamb wave generation, propagation and detection for an air coupled robotic scanner', Ultrasonics, vol. 51, issue 3, pp. 258-269, 2011.

[14] Friedrich, M., Pierce, S.G., Galbraith, W. and Hayward. G., 'Data fusion in automated robotic inspection systems', Insight-Non-Destructive Testing and Condition Monitoring, vol. 50, no. 2, pp. 88-94, 2008.

[15] Fabien Tache. Robot Locomotion and Localization on 3D Complex-Shaped Structures. PhD thesis, ETH Zurich, 2010. 48

[16] Katrasnik, J.; Pernus, F.; Likar, B., "A Survey of Mobile Robots for Distribution Power Line Inspection," in Power Delivery, IEEE Transactions on , vol.25, no.1, pp.485-493, Jan. 2010

[17] A. Correll, N. Martinoli. Multirobot inspection of industrial machinery. Robotics & Automation Magazine, IEEE, 16:103{112, 2009.

[18] A. Breitenmoser, H. Sommer, R. Siegwart, Adaptive Multi–Robot Coverage of Curved Surfaces, Distributed Autonomous Robotic Systems, Volume 104, Springer Tracts in Advanced Robotics pp 3-16

[19] A. Correll, N. Martinoli. Multirobot inspection of industrial machinery. Robotics & Automation Magazine, IEEE, 16:103{112, 2009.

[20] C. Mineo, B. Wright, I. Nicholson, I. Cooper, G. Pierce, PAUT inspection of complex shaped composite materials through 6 DOFs robotic manipulators, Insight Journal, Volume 57, No 3, March 2015,

[21] Alstom Inspection Robotics, http://www.inspection-robotics.com Accessed Nov. 2015.

[22] Silverwing NDT Scoprion, http://www.silverwingndt.com/ultrasonic-testing/scorpion-remote-ut-thickness-measurements, Accessed Nov. 2015.

[23] Techitest Ceta, http://www.tecnitestndt.com/wall-crawler/, Accessed

Nov. 2015..

[24] Galceran, E. and Carreras, M., 'A survey on coverage path planning for robotics, Robotics and Autonomous Systems', vol. 61, issue 12, pp. 1258-1276, Dec. 2013.

[25] Atkar, P., Greenfield, A.L., Conner, D.C., Choset, H. and Rizzi, A., 'Uniform coverage of automotive surface patches', The International Journal of Robotics Research, vol. 24, no. 11, pp. 883-898, Nov. 2005.

[26] Hert, S., Tiwari, S. and Lumelsky, V., 'A terrain-covering algorithm for an auv', Autonomous Robots 3, pp. 91-119, 1996.

[27] Acar, E.U., Choset, H., Zhang, Y. and Schervish, M., 'Path planning for robotic demining: robust sensor-based coverage of unstructured environments and probabilistic methods', International Journal of Robotics Research, vol. 22, pp. 441-466, 2003.

[28] Cao, Z.L., Huang, Y. and Hall, E.L., 'Region filling operations with random obstacle avoidance for mobile robotics', Journal of Robotic Systems, vol. 5, issue 2. pp. 87-102, 1988.

[29] Choset, H., 'Coverage for robotics—a survey of recent results', Annals of Mathematics and Artificial Intelligence, vol. 31, issue 1-4, pp. 113-126, 2001.

[30] Atkar, P., Greenfield, A, L., Conner, D. C., Choset, H. and Rizzi, A., 'Uniform Coverage of Automotive Surface Patches', The International Journal of Robotics Research, vol. 24, no. 11, pp. 883- 898, Nov. 2005.

[31] Olivieri, P., Birglen, L., Maldague, X. and Mantegh I., 'Coverage path planning for eddy current inspection on complex aeronautical parts', Robotics and Computer-Integrated Manufacturing, vol. 30, issue 3, pp. 305-314, June 2014,

[32] Sattar, T.P. and Brenner, A.A. 'Robotic system for inspection of test objects with unknown geometry using NDT methods' Industrial Robot: An International Journal, vol. 36, issue. 4, pp. 340–343, 2009.

[33] Weihua Sheng; Hongjun Chen; Ning Xi, "Navigating a Miniature Crawler Robot for Engineered Structure Inspection," Automation Science and Engineering, IEEE Transactions on , vol.5, no.2, pp.368,373, April 2008

[34] Englot, B.H. and Franz S. TI 'Three-dimensional coverage planning for an underwater inspection robot' International Journal of Robotics Research, vol. 32 issue: 9-10, pp. 1048-1073, 2013.

[35] C. Mineo, S. G. Pierce, P. I. Nicholson, B. Wright, I. Cooper, Robotic path planning for non-destructive testing - a custom MATLAB toolbox approach, Robotics and Computer-Integrated Manufacturing Journal – Accepted for publication on 18th May 2015.

[36] Hoff, E.B. and Sarker, B. R., 'An overview of path design and dispatching methods for automated guided vehicles', Integrated Manufacturing Systems, vol. 9 issue. 5, pp. 296-307, 1998.

[37] Jin, J. and Tang L., 'Coverage path planning on three-dimensional terrain for arable farming' Journal of Field Robotics, vol. 28, issue 3, pp. 424-440, 2011.

[38] Donald, B.R., 'Motion Planning with Six Degrees of Freedom', Massachusetts Institute Technology Artificial Intelligence Laboratory, Technical Report AIM-791, 1984.

[39] Brooks, R. A., 'Solving the find path problem by representing free space as generalized cones' A.I Memo No 674, Massachusetts Institute Technology, May 1982.

[40] Kambhampati, S. and Davis, L.S., 'Multiresolution path planning for mobile robots', Robotics and Automation, IEEE Journal of , vol.2, no.3, pp.135-145, Sep. 1986

[41] Babel L., 'Flight path planning for unmanned aerial vehicles with landmark-based visual navigation', Robotics and Autonomous Systems, vol. 62, issue 2, pp 142-150, Feb. 2014.

[42] Barrientos, A., Colorado, J., Cerro, J. d., Martinez, A., Rossi, C., Sanz, D. and Valente, J., 'Aerial remote sensing in agriculture: A practical approach to area coverage and path planning for fleets of mini aerial robots', Journal of Field Robotics, vol. 28, pp. 667-689, 2011.

[43] BL Luk, KP Liu, AA Collie, DS Cooke, and S. Chen. Tele-operated climbing and mobile service robots for remote inspection and maintenance in nuclear industry. Industrial Robot: An International Journal, 33(3):194{204, 2006.

[44] Fahimi, F., Autonomous Robots Modeling, Path Planning, and Control, Springer US, 2009.

[45] Pease W, 'An automatic machine tool' Scientific American, issue Sep., pp. 101-115, 1952.

[46] Thyer, G. E., Computer numerical control of machine tools, Industrial Press, Incorporated, 1988.

[47] Dragomatz, D. and Mann, S., 'A classified bibliography of literature on NC milling path generation', Computer-Aided Design, vol. 29, issue 3, pp. 239-247, Mar. 1997.

[48] http://cncsimulator.info/OnlineHelp/OnlineHelp.html?PocketMilling.html, Accessed Feb. 2014.

[49] Yong Seok Suh, Kunwoo Lee, NC milling tool path generation for arbitrary pockets defined by sculptured surfaces, Computer-Aided Design, Volume 22, Issue 5, June 1990, Pages 273-284.

[50] Marshall S., Griffiths G.J., 'A survey of cutter-path construction techniques for milling machines' International Journal of Production Research, Volume 32, Issue 12, 1994

[51] Xu, X.W., Wang, L. and Rong, Y., 'STEP-NC and function blocks for interoperable manufacturing', Automation Science and Engineering, IEEE Transactions on , vol. 3, no. 3, pp. 297- 308, Jul. 2006.

[52] Neto, P. and Mendes, N., 'Direct off-line robot programming via a common CAD package', Robotics and Autonomous Systems, vol. 61, issue 8, pp. 896-910, Aug. 2013.

[53] Chan, S.F. and Kwan R., 'Post-processing methodologies for off-line robot programming within computer integrated manufacture', Journal of Materials Processing Technology, vol. 139, issues 1-3, Aug. 2003.

[54] Gadow, R., Candel, A. and Floristán, M., 'Optimized robot trajectory generation for thermal spraying operations and high quality coatings on free-form surfaces', Surface and Coatings Technology, vol. 205, issue 4, pp. 1074-1079, Nov. 2010.

[55] Dobie, G., Galbraith, W., MacLeod, C.N., Summan, R., Pierce, S.G. and Gachagan, A., 'Automatic ultrasonic robotic array', 40th Annual Review of Progress in Quantitative Nondestructive Evaluation, pp. 1881-1888, Baltimore, Maryland, USA, 2013

[56] Analog Devices, http://www.analog.com/, Accessed Nov. 2015.

[57] KNJN LLC, http://www.knjn.com/, Accessed Nov. 2015.

[58] VICON Motion Capture Systems, http://www.vicon.com/, Accessed Nov. 2015

[59] Gordon Dobie. Ultrasonic Sensor Platforms for Non-Destructive Evaluation. PhD thesis, University of Strathclyde, 2010. 4, 215

[60] Nelligan, T. ' An Introduction to Ultrasonic Thicnkess Gauging – Olympus'. www.olympus-ims.com, Accessed Nov. 2015

[61] Drury, J.C., 'Corrosion Monitoring and Thickness Measurement - What are we doing wrong?', Insight. 39(1) : 17-20; 1997

[62] Porter, R.,'Non-destructive Examinations Applied to Hull Structure' Proceedings of the 7th European Conference on Non-Destructive Testing, 26-29 May 1998,

[63] Weire,D.R., Pardini, A.F., 'Evaluation of UT Wall Thickness Measurements and Measurement Methodology'', Pacific Northwest National Laboratory, www.pnnl.gov, Accessed Nov. 2015.

[64] Marietta NDT, http://www.marietta-ndt.com, Accessed Nov. 2015.

[65] H. Schempf, E. Mutschler, A. Gavaert, G. Skoptsov, and W. Crowley. Visual and Nondestructive Evaluation Inspection of Live Gas Mains using the ExplorerTM family of Pipe Robots. Journal of Field Robotics, 27(3):217, 2010. 47

[66] TS White, R. Alexander, G. Callow, A. Cooke, S. Harris, and J. Sargent. A Mobile Climbing Robot for High Precision Manufacture and Inspection of Aerostructures. The International Journal of Robotics Research, 24(7):589, 2005. 48

[67] R. Summan, S.G. Pierce, C.N. Macleod, G. Dobie, T. Gears, W. Lester, P. Pritchett, P. Smyth, Spatial calibration of large volume photogrammetry based metrology systems, Measurement, Volume 68, May 2015, Pages 189-200, ISSN 0263-2241,